Available online at www.sciencedirect.com
SCIENCE DIRECT®
Applied Acoustics 67 (2006) 511–528
applied acoustics
www.elsevier.com/locate/apacoust

Optimal design of FIR beamformer with frequency invariant patterns

Shefeng Yan *

Institute of Acoustic Engineering, Northwestern Polytechnical University, P.O. Box #19, Xi'an, Shaanxi 710072, China

Received 31 May 2005; received in revised form 9 August 2005; accepted 22 September 2005
Available online 21 November 2005

Abstract

Two approaches to the optimal design of FIR beamformers with frequency invariant patterns using second-order cone programming (SOCP) are proposed. The first approach is a two-step method, which is implemented via separately optimal array pattern synthesis and optimal FIR filters design. The array weights for each frequency bin within the working frequency band are designed to insure that the array patterns approximate the reference ones. And the FIR filter corresponding to each sensor is designed to insure that the frequency responses approximate the array weights. The second approach is a direct method, in which the beam response is expressed as a linear function of FIR filter tap weights and the filters are designed by jointly optimizing the spatial and frequency responses to achieve the desired array patterns. All the optimal design problems (array pattern synthesis, FIR filter design and joint optimization) are formulated as the SOCP, which can be solved efficiently using the well-developed interior-point methods. Results of computer simulations and lake experiment for a twelve-element semicircular array confirm satisfactory performance of the two approaches proposed in this paper.

Keywords: Underwater acoustics; FIR beamformer; Frequency invariant patterns; Second-order cone programming

* Tel.: +86 29 88495826.
E-mail address: shefengyan@hotmail.com.

0003-682X/$ - see front matter © 2005 Elsevier Ltd. All rights reserved.
doi:10.1016/j.apacoust.2005.09.008

1. Introduction

In broadband array signal processing, it is well known that as the frequency increases, the beamwidth of conventional beamformers decreases. This beamwidth variation as a function of frequency will subject the signals incident on the outer portions of the main beam to low-pass filtering and lead to distorted signal spectra. The so-called frequency invariant beamformer (FIB) technique is required as a remedy.

An FIB is a beamformer in which the response is (approximately) constant over some design bandwidth. An approach of design FIB has been proposed in [1,2]. In [1], an analog technique based on approximating an ideal continuous aperture was presented. The FIB is obtained by using dilation filters [2] at array elements before weighting. However, the frequency invariant beam patterns may not be achieved for an arbitrary array. Moreover, the approach design weights to insure that the beam response approximates the reference one in both the mainlobe and the sidelobe areas. In fact, only the beam patterns within the mainlobe area are of interest. This approach leads to larger error since the approximation in the sidelobe areas is not required. Only the sidelobe peaks need guarantee to be below the prescribed threshold value.

FIR broadband beamformers are implemented by placing a tapped delay line or FIR filter at the output of each sensor [3–5]. An FIR filter structure for narrowband beamformer was presented by Zhang and Ma [6]. Based on this methodology, we can develop the FIR narrowband beamforming to a broadband one. Our design methods for FIR broadband FIB can consist of two parts: array pattern synthesis and design of FIR filters with frequency response derived from the array weights. The FIR beamformer via optimal array pattern synthesis and optimal FIR filter design is termed "two-step method" in this paper. Firstly, the working frequency band is decomposed into a number of narrow band frequency bins and then the array weights for each frequency bin are designed so that the beam patterns approximate the reference ones via array pattern synthesis methods. Secondly, the FIR filters for each sensor are designed to insure that the magnitude and phase responses approximate the array weights of the sensor. Finally, each sensor feeds an FIR filter and the filter outputs are summed to produce the FIB output time series.

A number of array pattern synthesis approaches existed in the literature [7–12]. Recent advances in convex optimization have motivated a class of algorithms for the array pattern synthesis problem [13,14]. As a development of convex optimization, second-order cone programming (SOCP) [15] has been exploited in robust beamforming [16,17] and sidelobes control beamforming [18]. In fact, the design of our FIB array weights for each frequency bin can also be formulated as a convex SOCP problem, which can be solved using the well-established interior-point methods (e.g., SDPT3 [19] or SeDuMi [20]). The SOCP approach allows us to determine whether the optimization problem is feasible and, in the case of an infeasible problem, to correct the optimization parameters to ensure feasibility.

The desired magnitude and phase response of the delay-line filters for a broadband beamformer can be derived from the array weights. Thus some optimal FIR filter design approaches can be used to design the delay-line filters. The design of FIR filters has been studied extensively and solved in a number of different ways. The key problems in these design methodologies are the choice of suitable design criterion and the computational technique used for optimizing the criterion chosen [21–28]. We have shown that the FIR filters design problem can also be rewritten in an equivalent form of the SOCP and solved easily in [29].

However, the above two-step design methods can only obtain the optimal solution for array pattern synthesis and FIR filter design separately. They cannot guarantee to obtain the global optimum solution for FIR broadband FIB. While joint optimization method proposed in this paper can provide the global optimum solution. The beam responses are jointly optimized to satisfy some spatial and frequency domain specifications by designing a set of FIR filters corresponding to the input channels. Firstly, we express the broadband beam response as a linear function of the tap weights of the set of FIR filters corresponding to the channels. Then, the design of FIR filters for FIB can also be formulated as the SOCP problem for solution. A preliminary description of our approach appeared in [30,31].

In formulating the SOCP, no assumption has been made on the gain and phase response or characteristics of the individual array elements. Therefore, our two approaches can be applied to an array of arbitrary shape with the characteristic of the array elements taken into consideration as long as one is able to model the array accurately.

The paper is organized as follows. Section 2 provides a brief review of SOCP. The fundamental theoretical framework of FIR broadband beamformer is presented in Section 3. Section 4 described the FIR broadband FIB approach via array pattern synthesis and FIR filters design, and presents the SOCP formulations for them. The SOCP-based algorithm for the joint optimization design of FIR broadband FIB is described in Section 5. In Sections 6 and 7, the simulations and the practical array processing results for FIR broadband FIB by the two approaches are presented, respectively. Section 8 contains our concluding remarks.

2. Second-order cone programming

SOCP, also known as conic quadratic programming, is a subclass of the well-structured convex programming problems where a linear function is minimized subject to a set of second-order cone constraints and possibly a set of linear equality constraints. The problem can be described as

$$\min_{\mathbf{y}} \quad \mathbf{b}^{\mathrm{T}}\mathbf{y}, \tag{1a}$$

$$\text{subject to } \|\mathbf{A}_i\mathbf{y}+\mathbf{b}_i\| \leqslant \mathbf{c}_i^{\mathrm{T}}\mathbf{y}+d_i, \quad i=1,2,\ldots,I, \tag{1b}$$

$$\mathbf{F}\mathbf{y}=\mathbf{g}, \tag{1c}$$

where $\mathbf{b}\in C^{\alpha\times 1}$, $\mathbf{y}\in C^{\alpha\times 1}$, $\mathbf{A}_i\in C^{(\alpha_i-1)\times\alpha}$, $\mathbf{b}_i\in C^{(\alpha_i-1)\times 1}$, $\mathbf{c}_i\in C^{\alpha\times 1}$, $\mathbf{c}_i^{\mathrm{T}}\mathbf{y}\in\Re, d_i\in\Re$, $\mathbf{F}\in C^{g\times\alpha}$, $\mathbf{g}\in C^{g\times 1}$ with $\Re$ and C being the set of real and complex numbers (or matrix), $\|\cdot\|$ denotes the Euclidean norm and $(\cdot)^{\mathrm{T}}$ denotes the transpose operation. The term "second-order cone" reflects the fact that each constraint in (1b) is equivalent to the following conic constraint:

$$\begin{bmatrix}\mathbf{c}_i^{\mathrm{T}}\\ \mathbf{A}_i\end{bmatrix}\mathbf{y}+\begin{bmatrix}d_i\\ \mathbf{b}_i\end{bmatrix}\in \mathrm{SOC}_i^{\alpha_i}, \tag{2}$$

where $\mathrm{SOC}_i^{\alpha_i}$ is the second-order cone in C^{α_i}. It is defined as

$$\mathrm{SOC}_i^{\alpha_i}\triangleq\left\{\begin{bmatrix}t\\ \mathbf{x}\end{bmatrix}\middle| t\in\Re, \mathbf{x}\in C^{(\alpha_i-1)\times 1}, \|\mathbf{x}\|\leqslant t\right\}, \tag{3}$$

where $\triangleq$ denotes the define operation.

The linear equality constraint in (1c) is equivalent to zero-cone constraint:

$$\mathbf{g} - \mathbf{F}\mathbf{y} \in \{\mathbf{0}\}^g, \tag{4}$$

where $\{\mathbf{0}\}^g$ is the zero cone which is defined as

$$\{\mathbf{0}\}^g \triangleq \{\mathbf{x} \mid \mathbf{x} \in C^{g\times 1}, \quad \mathbf{x} = \mathbf{0}\}. \tag{5}$$

From Eq. (1), it is evident that SOCP includes the linear programming and the convex quadratic programming as its special cases. The problem in Eq. (1) can be solved efficiently using an SOCP solver provided, for example, by SeDuMi, which allows both real and complex valued entries. On the other hand, SOCP itself is a subclass of semidefinite programming (SDP) for that the second-order cone constraint in (1b) is equivalent to a linear matrix inequality:

$$\begin{bmatrix} (\mathbf{c}_i^{\mathrm{T}}\mathbf{y} + d_i)\mathbf{I} & \mathbf{A}_i\mathbf{y} + \mathbf{b}_i \\ (\mathbf{A}_i\mathbf{y} + \mathbf{b}_i)^{\mathrm{T}} & \mathbf{c}_i^{\mathrm{T}}\mathbf{y} + d_i \end{bmatrix} \succeq 0, \tag{6}$$

where $\mathbf{I}$ is a identity matrix and "$\succeq$" denotes that a matrix is semidefinite.

Though SOCP is less general than SDP, interior-point methods that solve the SOCP problem in (1) directly have a much better worst-case complexity than an equivalent SDP method. The number of iterations to decrease the duality gap to a constant fraction of itself is bounded above by $O(\sqrt{I})$ for the SOCP algorithm, and by $O(\sqrt{\sum_i \alpha_i})$ for the SDP algorithm (see [32]). More importantly in practice, the amount of computation per iteration is $O(\alpha^2 \sum_i \alpha_i)$ for the SOCP algorithm and $O(\alpha^2 \sum_i \alpha_i^2)$ for the SDP [15].

3. Principle of FIR broadband beamformer

Consider an array of N sensors with arbitrary shapes and element directivities, the array pattern (which we sometimes refer to as "beam response" in this paper) in the direction θ at frequency f is

$$p(\theta, f) = \mathbf{w}^{\mathrm{T}}(f)\mathbf{v}(\theta, f) = \mathbf{v}^{\mathrm{T}}(\theta, f)\mathbf{w}(f), \tag{7}$$

where $\mathbf{v}(\theta,f) = [v_1(\theta,f), v_2(\theta,f), \ldots, v_N(\theta,f)]^{\mathrm{T}}$ is the array response vector of angle θ and frequency f, and $\mathbf{w}(f) = [w_1(f), w_2(f), \ldots, w_N(f)]^{\mathrm{T}}$ is the weight vector at frequency f.

Without loss of generality, we assume that the source signals have finite bandwidth, i.e., the working frequency band (or passband) $F_K \triangleq [F_{\mathrm{L}}, F_{\mathrm{U}}] \subset F$, where F_{L} and F_{U} are the low and up bound frequency, respectively, and $F \triangleq [0, f_s/2]$ with f_s being the sampling frequency. The stopband is F_P and the transition band is F_T, so $F = F_K \cup F_T \cup F_P$. We can discretize the passband, the transition band and the stopband using a finite number of frequencies $f_k \in F_K$, $(k = 1,2,\ldots,K)$, $f_t \in F_T$ $(t = 1,2,\ldots,T)$ and $f_p \in F_P$ $(p = 1,2,\ldots,P)$. The frequencies are often uniformly spaced. There is a tradeoff between design precision and the number of discretization. For more points, it would lead to better precision but longer computation time and vice versa.

The FIR broadband beamformers are implemented by placing an FIR filter at the output of each sensor. It can be stated as finding if it exists, a set of FIR filters with impulse response

$$\mathbf{h}_n = [h_{n0}, h_{n1}, \ldots, h_{n(L-1)}]^{\mathrm{T}}, \quad n = 1, 2, \ldots, N, \tag{8}$$

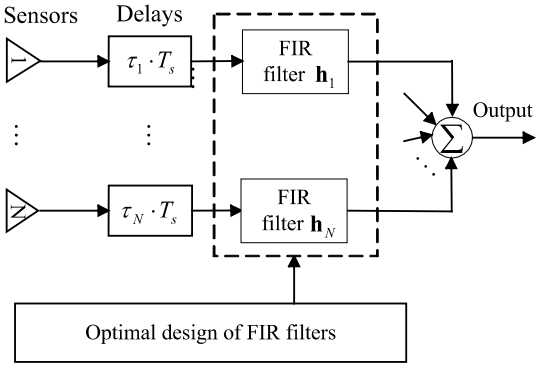

Fig. 1. FIR broadband beamformer structure.

whose response at frequency $f_k(k = 1,2,\ldots,K)$ is (approximately) equal to $w_n(f_k)$, i.e.,

$$\widetilde{H}_{n,d}(f_k) = w_n(f_k), \quad k = 1,2,\ldots,K, \;\; n = 1,2,\ldots,N, \tag{9}$$

where L in (8) is the length of filter $\mathbf{h}_n$. The filter tap weights are chosen to achieve the desired frequency response derived from the broadband array weights $\mathbf{w}$.

The design of FIR filters for broadband beamformer, however, is a little different from the general FIR filter design problem. It is well known that the group delay (unit in taps) of an FIR filter of length L is nearly $\zeta = (L-1)/2$ [21]. If the group delay of the desired FIR filter close to ζ, the design precision will increase. We first consider the array with pre-steering delays. Thus, we can rewrite the array weights as

$$w_n(f_k) = \exp[\mathrm{j}2\pi f_k \; \mathrm{int}(\zeta)T_\mathrm{s}] \cdot w_n(f_k) \exp[-\mathrm{j}2\pi f_k \; \mathrm{int}(\zeta)T_\mathrm{s}], \tag{10}$$

where int(·) denotes round towards nearest integer and $T_\mathrm{s} = 1/f_\mathrm{s}$ is the sampling interval. The first part of (10) can be implemented easily by integral delay of $-\mathrm{int}(\zeta)$ taps and the second part by an FIR filter. Thus, the desired frequency response of FIR filters is the second part of (10), i.e., $w_n(f_k)\exp[-\mathrm{j}2\pi f_k \; \mathrm{int}(\zeta)T_\mathrm{s}]$.

For the more general arrays without pre-steering delays, we assume the needed pre-steering delay for channel n is ς_n (unit in taps). The array weight can be thus rewritten as

$$w_n(f_k) = \exp[\mathrm{j}2\pi f_k \; \mathrm{int}(\zeta - \varsigma_n)T_\mathrm{s}] \cdot w_n(f_k) \exp[-\mathrm{j}2\pi f_k \; \mathrm{int}(\zeta - \varsigma_n)T_\mathrm{s}]. \tag{11}$$

The first part of (11) can be implemented by integral delay of $\tau_n = \mathrm{int}(\varsigma_n - \zeta)$ taps (when it is minus, a plus integral number can be added for all channels), and the second part by an FIR filter. Thus, the desired frequency response of FIR filters corresponding to the input channel n is

$$H_{n,d}(f_k) = w_n(f_k) \exp(\mathrm{j}2\pi f_k \tau_n T_\mathrm{s}), \quad k = 1,2,\ldots,K, \;\; n = 1,2,\ldots,N. \tag{12}$$

As a result, the FIR broadband beamformer structure is shown in Fig. 1.

4. FIB via optimal array pattern synthesis and optimal FIR filter design

4.1. Optimal array pattern synthesis

Let $p_d(\theta)$ be the desired array response in the direction θ. The array pattern synthesis problem is then stated as follows:

Find the weight vector $\mathbf{w}(f_k)$ such that

$$p(\theta, f_k) \approx p_d(\theta) \text{ for all } \theta \in \Theta_{\mathrm{ML}} \text{ and } f_k \in F_K,$$

where Θ_{ML} denotes the mainlobe areas.

How well $p(\theta,f_k)$ approximates $p_d(\theta)$ can be measured in several ways. Typical measures are the peak error across Θ_{ML}, or the mean-squared error over Θ_{ML}.

A number of array pattern synthesis approaches existed in the literature. A well-known solution was given by Dolph [7] for uniform linear arrays using the theory of Chebyshev polynomials. The designed pattern, known as the Dolph–Chebyshev pattern, has the property of the minimum sidelobe level for a given mainlobe width. However, the Dolph–Chebyshev method is only applicable for uniform linear arrays and cannot be applied for non-uniform arrays or arrays with unequal elements. For arrays with arbitrary shapes and element patterns, several algorithms have been developed to optimally design weights by formulating pattern synthesis problems as quadratic programming problems where the sum of the squared synthesis error between the synthesized pattern and the desired pattern is minimized [8–12]. However, in all these approaches, the design problem is implemented adaptively or recursively. The convergence of the iterations in general cannot be guaranteed. Furthermore, the quadratic programming approach leads to larger error in mainlobe areas because the approximation in sidelobe areas is not required. Since, in many cases, we are only interested in controlling the sidelobe peaks.

SOCP approach presented in this paper, however, leads to more flexible designs. It design array weights for each specific frequency bin within the working frequency band $[F_{\mathrm{L}},F_{\mathrm{U}}]$ so that beam response approximates the reference response by minimizing the peak error or mean-squared error within the mainlobe areas while controlling the sidelobe peaks.

At the same time, white noise gain constraint (WNC) can be used to improve the beamformer robustness against random errors in array characteristics [17,33]. That is, the norm of array weight vectors is bounded by some known constant $\gamma > 0$:

$$\|\mathbf{w}(f_k)\| \leqslant \gamma, \quad f_k \in F_K, \ \ k = 1, 2, \ldots, K.$$

Let $\theta_s \in \Theta_{\mathrm{SL}}$ $(s = 1,\ldots,S)$ and $\theta_m \in \Theta_{\mathrm{ML}}$ $(m = 1,\ldots,M)$ be chosen (uniform or non-uniform) grid that approximates the sidelobe areas Θ_{SL} and mainlobe areas Θ_{ML} using a finite number of angles, respectively. The array pattern synthesis problems for each frequency bin f_k according to the least-squares criteria can be stated as (omitting the f_k term temporarily):

$$\begin{aligned} \min_{\mathbf{w}} \quad & \left(\sum_{m=1}^{M} \lambda_m |p_d(\theta_m) - p(\theta_m)|^2 \right), \quad \theta_m \in \Theta_{\mathrm{ML}}, \ \ m = 1, \ldots, M, \\ \text{subject to } & |p(\theta_s)| \leqslant \delta, \quad \theta_s \in \Theta_{\mathrm{SL}}, \quad s = 1, \ldots, S, \\ & \|\mathbf{w}\| \leqslant \gamma, \end{aligned} \tag{13}$$

where λ_m is a non-negative weighting coefficient and δ is the prescribed sidelobe level. The prescribed sidelobes value can also be set to vary with angle.

The array pattern synthesis problems according to the minimax criteria in which the peak error across the mainlobe areas is minimized while controlling the sidelobe peaks can be stated as:

$$\begin{aligned} \min_{\mathbf{w}} \quad & \max \lambda_m |p_d(\theta_m) - p(\theta_m)|, \quad \theta_m \in \Theta_{\mathrm{ML}}, \ m = 1, \ldots, M, \\ \text{subject to} \quad & |p(\theta_s)| \leqslant \delta, \quad \theta_s \in \Theta_{\mathrm{SL}}, \quad s = 1, \ldots, S, \\ & \|\mathbf{w}\| \leqslant \gamma. \end{aligned} \tag{14}$$

Both the least-squares criteria and the minimax criteria used in array pattern synthesis problems can be formulated as the SOCP for solution. And the latter is easier than the former. Take the optimization problem (13) as an example. Introducing a set of new scalar non-negative variables ε_m, $m = 1, \ldots, M$, it is easy to express the original problem (13) as

$$\min_{\mathbf{w}} \quad \sum_{m=1}^{M} \lambda_m \varepsilon_m, \tag{15a}$$

$$\text{subject to} \quad |p_d(\theta_m) - \mathbf{v}^{\mathrm{T}}(\theta_m)\mathbf{w}|^2 \leqslant \varepsilon_m, \quad \theta_m \in \Theta_{\mathrm{ML}}, \ m = 1, \ldots, M, \tag{15b}$$

$$|\mathbf{v}^{\mathrm{T}}(\theta_s)\mathbf{w}| \leqslant \delta, \quad \theta_s \in \Theta_{\mathrm{SL}}, \ s = 1, \ldots, S, \tag{15c}$$

$$\|\mathbf{w}\| \leqslant \gamma. \tag{15d}$$

For the quadratic inequality constraint (15b), we have

$$\begin{aligned} |p_d(\theta_m) - \mathbf{v}^{\mathrm{T}}(\theta_m)\mathbf{w}|^2 \leqslant \varepsilon_m &\iff |2p_d(\theta_m) - 2\mathbf{v}^{\mathrm{T}}(\theta_m)\mathbf{w}|^2 \leqslant 4\varepsilon_m \\ &\iff 2p_d(\theta_m) - 2\mathbf{v}^{\mathrm{T}}(\theta_m)\mathbf{w}|^2 + 1 + \varepsilon_m^2 - 2\varepsilon_m \leqslant 1 + \varepsilon_m^2 + 2\varepsilon_m \\ &\iff \left\| \begin{matrix} 2p_d(\theta_m) - 2\mathbf{v}^{\mathrm{T}}(\theta_m)\mathbf{w} \\ \varepsilon_m - 1 \end{matrix} \right\|^2 \leqslant (\varepsilon_m + 1)^2 \\ &\iff \left\| \begin{matrix} 2p_d(\theta_m) - 2\mathbf{v}^{\mathrm{T}}(\theta_m)\mathbf{w} \\ \varepsilon_m - 1 \end{matrix} \right\| \leqslant \varepsilon_m + 1. \end{aligned} \tag{16}$$

Define $\mathbf{y} = [\varepsilon_1, \varepsilon_2, \ldots, \varepsilon_M, \mathbf{w}^{\mathrm{T}}]^{\mathrm{T}}$ and $\mathbf{b} = [\lambda_1, \lambda_2, \ldots, \lambda_M, \mathbf{0}_{1\times N}]^{\mathrm{T}}$, where $\mathbf{0}_{1\times M}$ is the $1 \times M$ dimensional zero vector. The optimization problem (15) becomes

$$\begin{aligned} \min_{\mathbf{y}} \quad & \mathbf{b}^{\mathrm{T}}\mathbf{y}, \\ \text{subject to} \quad & \left\| \begin{bmatrix} 2p_d(\theta_m) \\ -1 \end{bmatrix} - \begin{bmatrix} \mathbf{0}_{1\times M} & 2\mathbf{v}^{\mathrm{T}}(\theta_m) \\ -\mathbf{q}^{\mathrm{T}}(m) & \mathbf{0}_{1\times N} \end{bmatrix} \mathbf{y} \right\| \leqslant 1 + \begin{bmatrix} \mathbf{q}^{\mathrm{T}}(m) & \mathbf{0}_{1\times N} \end{bmatrix} \mathbf{y}, \quad m = 1, \cdots, M, \\ & \left| [\mathbf{0}_{1\times M} \quad \mathbf{v}^{\mathrm{T}}(\theta_s)]\mathbf{y} \right| \leqslant \delta, \quad s = 1, \cdots, S, \\ & \|[\mathbf{0}_{N\times M} \quad \mathbf{I}_{N\times N}]\mathbf{y}\| \leqslant \gamma, \end{aligned} \tag{17}$$

where $\mathbf{q}(m)$ is a column vector of length M with the mth element be 1 and others be zeros, i.e., $\mathbf{q}(m) = [\, q_1, q_2, \cdots, q_i, \cdots, q_M]^{\mathrm{T}}$, with $q_i = \begin{cases} 0 & i \neq m, \\ 1 & i = m. \end{cases}$

The optimization problem (17) is now in the form of SOCP as in Eq. (1). After solving the optimization problem (17) using SeDuMi MATLAB toolbox, the vector $\mathbf{y}$ contains both the optimal weight vector $\mathbf{w}$ and the achieved error within the mainlobe areas. With the similar procedure, the optimal array pattern synthesis problem (14) can also be formulated as the SOCP and solved.

4.2. Optimal FIR filter design

The desired frequency response of FIR filters for FIB can be derived from the array weights by Eq. (12). In this section, we consider the optimal design problem of FIR filter corresponding each channel.

Just like the optimal array pattern synthesis problem, optimal FIR filter design has been studied extensively and solved in a number of different ways. Various approximation methods can be developed by considering different definitions of error measure. Commonly used definitions are peak error (L_∞-norm) [21,22], mean-squared error (L_2-norm) [23,24] or the combination of them [25–28].

Consider that only the working frequency band F_K is of interest for our FIR filter design problem, the error measure minimization only to be carried out over the working frequency band while suppressing the stopband. In what follows, we show that the design of FIR filters for which the weighted least square error is minimized subject to maximum error constraints can also be formulated as a SOCP problem for solution. Using the proposed approach, a tradeoff can be achieved in terms of passband ripple and stopband level.

The complex frequency response of an FIR filter of length L and impulse response $\mathbf{h} = [h_0, h_1, \ldots, h_{L-1}]^{\mathrm{T}}$ is given by

$$H(f) = \sum_{l=0}^{L-1} h_l \exp(-\mathrm{j}l2\pi f/f_s) = \mathbf{e}^{\mathrm{T}}(f)\mathbf{h}, \tag{18}$$

where $\mathbf{e}(f) = [1, \mathrm{e}^{-\mathrm{j}2\pi f/f_s}, \ldots, \mathrm{e}^{-\mathrm{j}(L-1)2\pi f/f_s}]^{\mathrm{T}}$.

Let $H_d(f)$ be the desired complex frequency response at frequency f corresponding to a channel (e.g., the nth channel. And we omit the n term temporarily here). The optimal weight vector $\mathbf{w}$ obtained from Section 4.1 is assigned to $H_d(f)$. The optimal FIR filter design problem according to the least-squares criteria can be stated as

$$\begin{aligned} &\min_{\mathbf{h}} \quad \left(\sum_{k=1}^{K} \lambda_k \left| H_d(f_k) - \mathbf{e}^{\mathrm{T}}(f_k)\mathbf{h} \right|^2 \right), \quad f_k \in F_K, \ \ k = 1, 2, \ldots, K, \\ &\text{subject to } |\mathbf{e}^{\mathrm{T}}(f_p)\mathbf{h}| \leqslant \beta, \quad f_p \in F_P, \ \ p = 1, 2, \ldots, P, \end{aligned} \tag{19}$$

where β is the prescribed stopband level.

Note that the FIR filter design problem (19) is similar to array pattern synthesis problem (13) in form except that tap weights here is real while array weight vector is complex there. An SOCP based solving process for FIR filter design can be found in our earlier paper [29].

5. FIB via joint optimization

The above two-step design methods for FIR broadband FIB can only obtain the optimal solution for array pattern synthesis and FIR filter design separately. However, they cannot guarantee to obtain the global optimum solution. A shortcoming of it is that it is not clear how to obtain the optimal value of the stopband level of the desired FIR filters based on the prescribed stopband level of broadband beamformer. Furthermore, the sidelobe area at transition frequency band is a "don't care" area, and the sidelobes at these areas are difficult to be controlled. In what follows, we further design the FIR filters directly by jointly optimizing the spatial and frequency domain responses of the broadband beamformer.

Let $\kappa_{n,k} = \exp[-\mathrm{j}2\pi f_k \tau_n \ T_s]$, from Eq. (12), we obtain

$$w_n(f_k) = H_{n,d}(f_k)\kappa_{n,k}, \quad k = 1, 2, \ldots, K, \ \ n = 1, 2, \ldots, N. \tag{20}$$

We assume that the impulse response of the FIR filter corresponding to channel n is $\mathbf{h}_n$. From Eq. (18), we obtain

$$H_{n,d}(f_k) = \mathbf{e}^{\mathrm{T}}(f_k)\mathbf{h}_n. \tag{21}$$

Thus

$$\mathbf{w}(f_k) = \left[\mathbf{e}^{\mathrm{T}}(f_k)\mathbf{h}_1\kappa_{1,k}, \ldots, \mathbf{e}^{\mathrm{T}}(f_k)\mathbf{h}_n\kappa_{n,k}, \ldots, \mathbf{e}^{\mathrm{T}}(f_k)\mathbf{h}_N\kappa_{N,k}\right]^{\mathrm{T}}. \tag{22}$$

From Eq. (7), we obtain

$$\begin{aligned} p(\theta, f_k) &= \mathbf{v}^{\mathrm{T}}(\theta, f_k)\mathbf{w}(f_k) \\ &= \mathbf{v}^{\mathrm{T}}(\theta, f_k)[\mathbf{e}^{\mathrm{T}}(f_k)\mathbf{h}_1\kappa_{1,k}, \ldots, \mathbf{e}^{\mathrm{T}}(f_k)\mathbf{h}_n\kappa_{n,k}, \ldots, \mathbf{e}^{\mathrm{T}}(f_k)\mathbf{h}_N\kappa_{N,k}]^{\mathrm{T}} \\ &= [v_1(\theta, f_k)\mathbf{e}^{\mathrm{T}}(f_k)\kappa_{1,k}, \ldots, v_n(\theta, f_k)\mathbf{e}^{\mathrm{T}}(f_k)\kappa_{n,k}, \ldots, v_N(\theta, f_k)\mathbf{e}^{\mathrm{T}}(f_k)\kappa_{N,k}] \\ &\quad \cdot [\mathbf{h}_1^{\mathrm{T}}, \ldots, \mathbf{h}_n^{\mathrm{T}}, \ldots, \mathbf{h}_N^{\mathrm{T}}]^{\mathrm{T}}. \end{aligned} \tag{23}$$

Define $\boldsymbol{\kappa}_k = [\kappa_{1,k}, \ldots, \kappa_{n,k}, \ldots, \kappa_{N,k}]^{\mathrm{T}}$ and $\tilde{\mathbf{h}} = [\mathbf{h}_1^{\mathrm{T}}, \ldots, \mathbf{h}_n^{\mathrm{T}}, \ldots, \mathbf{h}_N^{\mathrm{T}}]^{\mathrm{T}}$, Eq. (23) takes the form

$$p(\theta, f_k) = \{[\mathbf{v}(\theta, f_k) \circ \boldsymbol{\kappa}_k] \otimes \mathbf{e}(f_k)\}^{\mathrm{T}}\tilde{\mathbf{h}}, \tag{24}$$

where $\circ$ denotes the Hadamard product of two vectors, i.e., correspond to the element-wise product, and $\otimes$ denotes the Kronecker product. We further define $\mathbf{u}(\theta, f_k) = [\mathbf{v}(\theta, f_k) \circ \boldsymbol{\kappa}_k] \otimes \mathbf{e}(f_k)$. Eq. (24) takes the form

$$p(\theta, f_k) = \mathbf{u}^{\mathrm{T}}(\theta, f_k)\tilde{\mathbf{h}}. \tag{25}$$

The broadband FIB problem consists of designing FIR filters for each channel so that beam responses over passband approximates the reference response within the mailobe areas while controlling the sidelobes and the array patterns over stopband. The broadband array pattern synthesis problem is then stated as follows:

Find the FIR filter impulse response $\tilde{\mathbf{h}}$ such that
$p(\theta, f) \approx p_d(\theta)$ for all $\theta \in \Theta_{\mathrm{ML}}$ and $f \in F_K$
and $|p(\theta, f)| \leqslant \xi$ for $\theta \in \Theta_{\mathrm{SL}}$ or $f \in F_P$,

where ξ is the prescribed sidelobe level. It can also be prescribed individually for various directions and frequencies.

For an FIR broadband beamformer, white noise gain constraint is to bound the norm of FIR filter impulse response to some known constant $\sigma > 0$:

$$\sum_{n=1}^{N} \|\mathbf{h}_n\|^2 \leqslant \sigma^2 \text{ or } \|\tilde{\mathbf{h}}\|^2 \leqslant \sigma^2. \tag{26}$$

Let $\theta_q (q = 1, \ldots, Q)$ be chosen grid that approximates the whole visible areas Θ over the stopband. The broadband array pattern synthesis problem can be represented as a minimax optimization problem

$$\begin{aligned} \min_{\tilde{\mathbf{h}}} \quad & \max\left(\lambda_m \left| p_d(\theta_m) - \mathbf{u}^{\mathrm{T}}(\theta_m, f_k)\tilde{\mathbf{h}}\right|\right), \quad m = 1, \ldots, M, \ k = 1, 2, \ldots, K \\ \text{subject to } & \mathbf{u}^{\mathrm{T}}(\theta_s, f_k)\tilde{\mathbf{h}}| \leqslant \xi, \quad s = 1, \ldots, S, \ k = 1, 2, \ldots, K, \\ & |\mathbf{u}^{\mathrm{T}}(\theta_s, f_t)\tilde{\mathbf{h}}| \leqslant \xi, \quad s = 1, \ldots, S, \ t = 1, 2, \ldots, T, \\ & |\mathbf{u}^{\mathrm{T}}(\theta_q, f_p)\tilde{\mathbf{h}}| \leqslant \xi, \quad q = 1, \ldots, Q, \ p = 1, 2, \ldots, P, \\ & \|\tilde{\mathbf{h}}\| \leqslant \sigma. \end{aligned} \tag{27}$$

The optimal design problem (27) is also convex and can be formulated as SOCP problem with the similar processing procedure as described in Section 4.1.

Note that after solving the optimization problem and obtaining the vector $\tilde{\mathbf{h}}$, the resulting FIR filters of our broadband beamformer corresponding to the channel n is given by its sub-vector $\mathbf{h}_n$.

6. Simulation results

The development in this paper is applicable to general volume arrays, and for simplicity, only planar array is considered in this paper and we assume that the elements are isotropic in this section. However, the generalization to three-dimensional array and arbitrary element patterns is straightforward.

To compare the performance of the "two-step method" and the "joint optimization method", the minimax criteria is used to both the array pattern synthesis and joint optimization problem. For the FIR filter design problem, the lease-squares criterion is used to show the flexibility of our SOCP approach.

Consider a semicircular hydrophone array of $N = 12$ sensors equally spaced on the circumference with a radius of 1.5 m. The diagram of the array is shown in Fig. 2.

We assume that the passband is $[F_L, F_U] = [928\ 1952\ \text{Hz}]$ that cover more than one-octave frequency band. The sampling frequency is $f_s = 6400$ Hz.

In this simulation, we would like to discretize the passband with uniform frequency bin of 64 Hz so there are total $K = 16$ frequency bins and the central frequencies of the 16 frequency bins are $\{f_k\}_{k=1}^{16} = 960, 1024, \ldots,$ and 1920 Hz, respectively.

The conventional (delay-and-sum) array patterns with look direction 90° at all the 16 central frequencies are shown in Fig. 3(a). It can be seen that the beamwidth varies with frequency and the sidelobe level is about −7.5 dB, which can be prohibitively high in many applications.

6.1. Optimal array pattern synthesis

We first consider the array without pre-steering delays. We take the conventional array pattern of 960 Hz in the mainlobe area as the reference array pattern, and 5 beam response points with the angle $\{\theta_m\}_{m=1}^{5} = \{72.5°, 80°, 90°, 100°, 107.5°\}$ are chosen as the desired beam responses. The sidelobe areas $\Theta_{SL} = [0°,65°] \cup [115°,180°]$ are chosen and a uniform

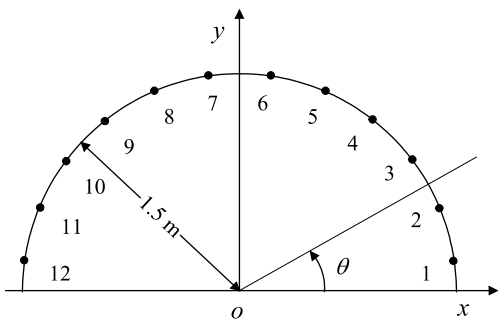

Fig. 2. The semicircular hydrophone array.

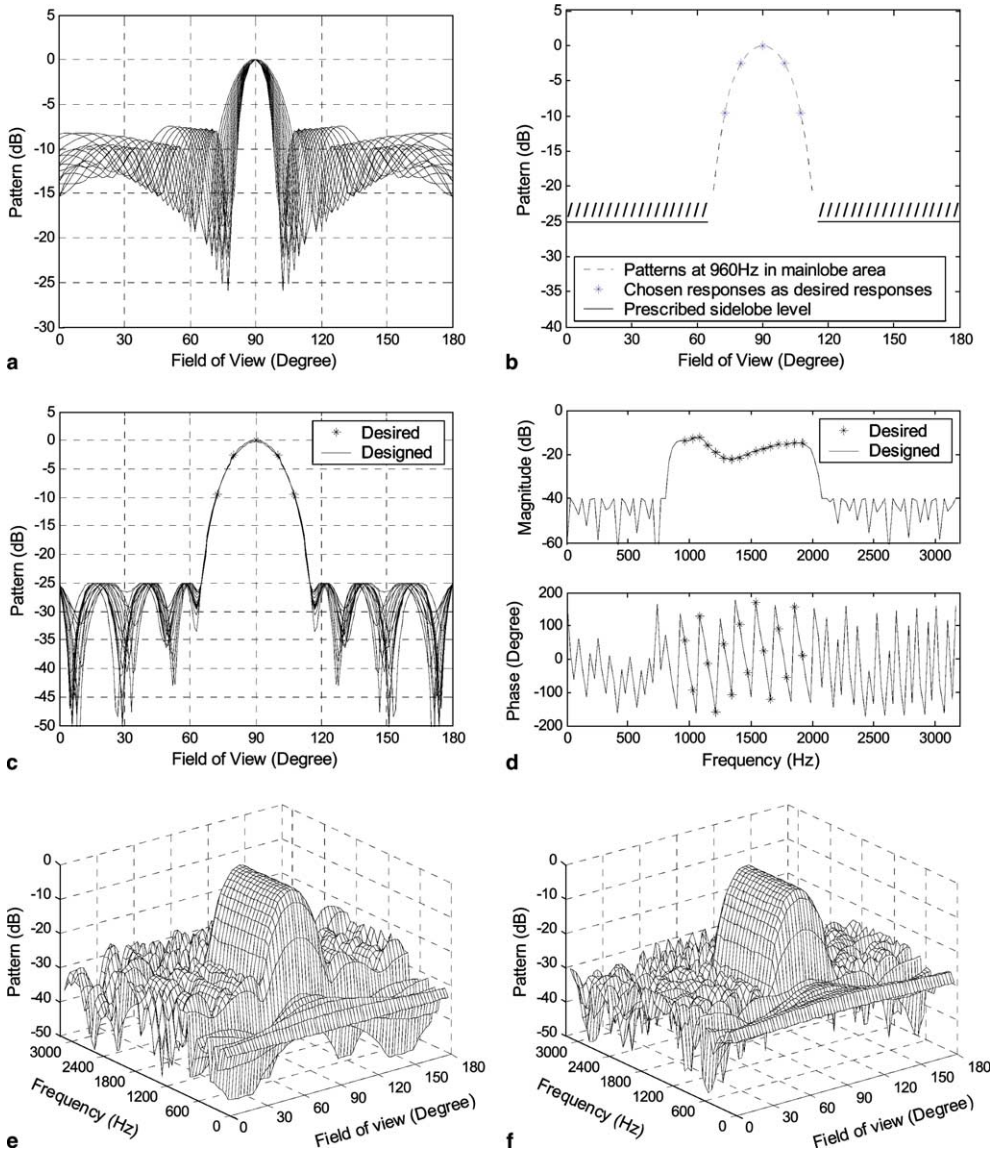

Fig. 3. Results of computer simulation for array without pre-steering delays: (a) conventional beam patterns at 16 frequencies within the passband; (b) desired beam responses and sidelobe level; (c) beam patterns using SOCP pattern synthesis method; (d) the desired and the designed frequency responses of FIR filter for No. 5 channel; (e) FIR broadband beam patterns by "two-step method"; (f) FIR broadband beam patterns by joint optimization method.

grid of 2.5° is used to obtain the angles $\theta_s(s = 1,\ldots,S)$. The prescribed sidelobe level is set to be -25 dB. The desired beam patterns within the mainlobe and the prescribed sidelobe level are shown in Fig. 3(b).

We use the array pattern synthesis method as describe in Eq. (14) to design the array weights for the semicircular array at the 16 frequencies provided that there are no array

errors. The error weighting coefficients are chosen to be $\lambda_m = 1$ ($m = 1,2,\ldots,5$) and the constraint on the weight vector norm is $\gamma = 0.7$. For each frequency bin, SOCP problem (14) is solved to get the array weights. The achieved beam patterns for the 16 central frequencies are plotted in Fig. 3(c). The peak error at all the 16 frequencies in passband and directions in the mainlobe areas is 0.029. From Fig. 3(c), it can be seen that all the 16 array patterns approximate to the desired array pattern in the mainlobe area with very little error and the sidelobes are strictly below the given specification (−25 dB). With the SOCP method, a set of satisfactory array patterns are obtained.

6.2. Design of FIR filter with Specified response

The desired frequency response of FIR filter is calculated from the array weights via Eq. (12) for each sensor. As an example, the desired magnitude and phase responses within the passband for No. 5 sensor is shown in Fig. 3(d) by "*". We design the FIR filters for broadband beamformer by solving the optimization problem (19). In this simulation, we assume that the length of the FIR filters is $L = 64$. The stopband F_p=[0,768 Hz] ∪ [2112,3200 Hz] are chosen and a uniform grid of 32 Hz is used to obtain the frequencies $f_p \in F_P$ ($p = 1,2,\ldots,P$). The error weighting coefficients are chosen to be $\lambda_k = 1$ ($k = 1,2,\ldots,16$), and the desired stopband level is −40 dB.

SOCP problem (19) is solved to get the FIR filters. The magnitude and phase responses of the designed FIR filter for No. 5 element are shown in Fig. 3(d) by solid line. The achievable root-mean-square error in the working frequency band is 0.0042. And the achieved stopband level is strictly below −40 dB. Form Fig. 3(d), it follows that the desired FIR filter can be designed with high precision and good performance against noise of stopband.

The FIR filters for other channels can also be designed according their array weights with the similar procedure. With the 12 FIR filters designed, the beam response as a function of frequency and angle can be calculated on a grid of points spaced every 64 Hz in frequency and 2.5° in angle. The achieved FIR broadband array patterns are shown in Fig. 3(e). The maximum peak error between the obtained beam responses and the desired ones in the passband and mainlobe areas is 0.032, which is still small and acceptable. The sidelobe level at the passband is about −23 dB and that at the transition band and stopband are −21 and −26 dB, respectively.

From the above simulations, we can find that the sidelobe level in the passband is a little higher than the specification since there exist some errors in designed filters. One disadvantage of the "two-step method" is how to choose the stopband level of the desired FIR filters based on the prescribed stopband level of FIR beamformer. Furthermore, the sidelobe area at transition band is a "don't care" area, and the sidelobes at these areas are difficult to be controlled. However, if the design requirement on the sidelobes is not very strict, the "two-step method" can satisfy applications-oriented requirements at most situations.

6.3. Design of FIR filter via joint optimization

We assume that both the prescribed sidelobe level and the beam response magnitude at stopband are −25 dB, the constraint on the norm of FIR filters tap weights in Eq. (26) is $\sigma = 0.30$ (in the case of "two-step method", the norm of total FIR filters tap weights is 0.31). The other parameters are set as the same as "two-step method".

Table 1
Performance of the FIR beamformers

Arrays	Pre-steering	Design methods	Sidelobe level (dB)	Peak error	$\|\tilde{\mathbf{h}}\|$	CPU time (s)
Nominal array	Without	Two-step	−21	0.032	0.31	10.5
	Without	Joint	−25	0.014	0.30	868
	With	Two-step	−23	0.031	0.32	11.8
	With	Joint	−25	0.014	0.30	1022
Practical array	Without	Two-step	−18	0.092	0.31	8.6
	Without	Joint	−25	0.020	0.30	481
	With	Two-step	−19	0.084	0.32	8.5
	With	Joint	−25	0.020	0.30	372

SOCP problem (27) is solved to get the FIR filters for all the 12 channels. The beam responses as a function of frequency and angle are calculated on a grid of points spaced every 64 Hz in frequency and 2.5° in angle. The achieved FIR broadband array patterns via joint optimization are shown in Fig. 3(f). The sidelobes and the beam response magnitude at stopband are strictly below the given specification (−25 dB).

The peak error between the obtained beam responses and the desired ones in the passband and mainlobe areas is 0.014, which is smaller than the "two-step method". Just as we desired, the broadband FIB has been implemented with satisfying beam patterns.

On the other hand, since there are much more optimization variables in the joint optimization method than those in the "two-step method", the computational complexity of joint optimization is much higher than that of the "two-step method". The joint optimization method offers improved design performance at the cost of increased amount of computation. The CPU time used on a Pentium 2.8 G for a MATLAB implementation of the algorithm to accomplish the designs are given in Table 1. The design performances of the FIR broadband beamformers by the two approaches are also presented in Table 1.

6.4. Array with pre-steering delays

In real situations, hydrophone array will be used with pre-steering to steer arbitrary direction. The FIR broadband beam patterns by the "two-step method" and the "joint optimization method" for the array with pre-steering delays are shown in Fig. 4. The simulation

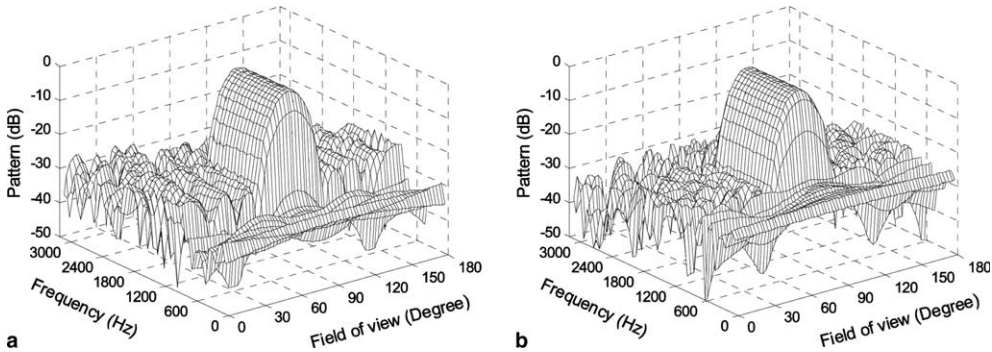

Fig. 4. Results of computer simulation for array with pre-steering delays: (a) FIR broadband beam patterns by "two-step method"; (b) FIR broadband beam patterns by joint optimization.

result on the array with pre-steering delays is somewhat similar to that on the array without pre-steering delays (see Table 1).

7. Experimental results on a practical array

In practical array, there are many error sources, such as the sensor sensitivity mismatch errors, the channel gain and phase mismatch errors, and the element position perturbation. Most of all, when these sensors are installed on the array, structural scattering and shadowing occurs, which results in very large direction-dependent array mismatch errors. As a result, the elements of practical array are non-isotropic. Fig. 5(a) shows a 24-element practical circular hydrophone array. The 12-element semicircular array used in this paper is just a half of the circular array.

The structural scattering and shadowing phenomena can be observed in Fig. 5(b). Fig. 5(b) shows the sampled time-domain waveforms collected from the 12 hydrophone channels by the use of a data acquisition system in a lake experiment. An omni-directional source transmits a sinusoidal signal with frequency of 960 Hz from the angle $\theta = 0°$. From

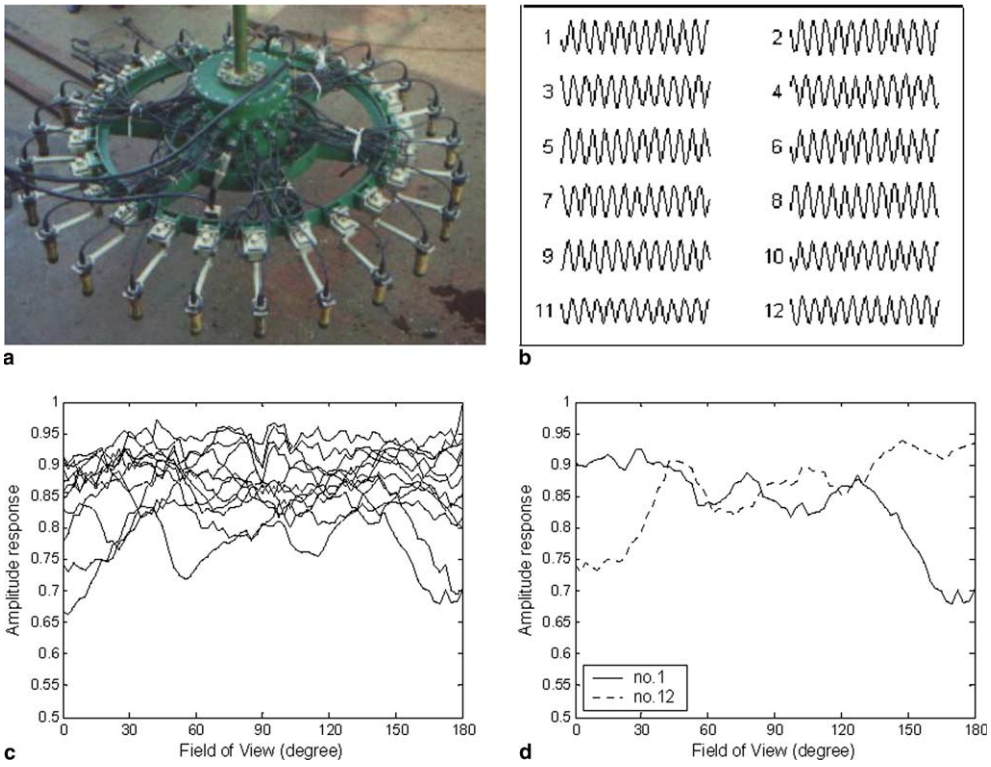

Fig. 5. Effect of mismatch array errors: (a) the construction drawing of a 24-element practical circular array. The 12-element semicircular array used in this paper is a half of the circular array; (b) waveforms sampled simultaneously at the 12 receiver channels reflecting the structural scattering and shadowing phenomena in the practical array; (c) element pattern distortion caused by structural shadowing and scattering: comparison of amplitude responses of all element patterns; (d) element pattern distortion caused by structural shadowing and scattering: comparison of patterns for a typical near element (No. 1) and a typical distant element (No. 12).

Fig. 5(b) it can be seen that the signals received by the elements towards the source (say No. 1 and No. 2 hydrophone) are stronger than those received by the elements away from the source (say No. 11 and No. 12 hydrophone). Unusual phase variation can also be observed from the waveform.

By fixing the position of the source and rotating the array around the centre axis of the semicircle, we can record the received waveform at different bearing angles. Using some spectrum analysis method (such as FFT, maximum likelihood method) we can estimate the spatial response vector at each bearing angle (see also [34]). This vector is called the array manifold vector. The practical element patterns (magnitude) can be plotted by using all measured array manifold vectors, as shown in Fig. 5(c) and (d).

In Fig. 5(c), we compare the amplitude responses of all element patterns as a function of the bearing angle θ. Severe direction-dependent mismatch errors can be noted. In the case of no array errors, all these curves should coincide and take a constant value of 1.0 over all bearing angle (i.e., omnidirectional). Fig. 5(d) compares the amplitude responses of the element patterns of a typical near element (No. 1 hydrophone) and a typical distant element (No. 12 hydrophone), from which the shadowing effect can be observed clearly.

The measured array manifold vectors for other frequencies can also be obtained by changing the frequency of the transmitting sinusoidal signal. In this experiment, the array manifold vectors at 31 frequencies (448, 512, . . . ,2368 Hz) are measured.

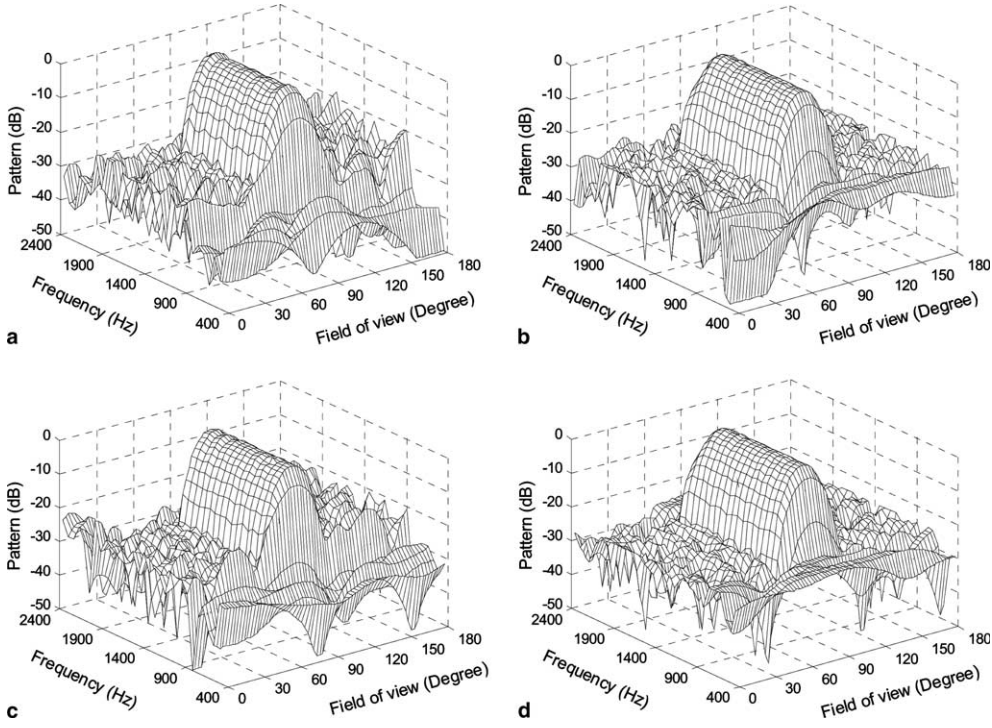

Fig. 6. Array patterns for imperfect array in a lake experiment: (a) array patterns by two-step method for array without pre-steering delays; (b) array patterns by joint optimization method for array without pre-steering delays; (c) array patterns by two-step method for array with pre-steering delays; (d) array patterns by joint optimization method for array with pre-steering delays.

Instead of using the theory array manifold vectors, we use the measured ones and keep other parameters the same as in Section 6 when designing the array patterns and the FIR filers. The FIR filters for FIR broadband FIB are designed by applying the ''two-step method'' and the joint optimization method, respectively. The broadband pattern synthesis technique was tested in the lake experiment. The FIR broadband FIB patterns by the ''two-step method'' and the ''joint optimization method'' for array without pre-steering delays are plotted in Fig. 6(a) and (b), respectively.

By comparing Fig. 6(b) with (a), it can be noted that the performance improvement is significant. The sidelobes in Fig. 6(a) is a little higher, especially at the transition band, while the sidelobes in Fig. 6(b) are strictly below the given specification (−25 dB). The peak error between the actual beam patterns by ''two-step method'' and the reference ones in the mainlobe areas over the passband is 0.092, while the peak error by the joint optimization is 0.020. The broadband beam patterns in Fig. 6(b) are much better than those in Fig. 6(a). However, the array patterns in Fig. 6(a) are also acceptable if the design requirement is not so strict. The advantage of the ''two-step method'' is that it has less computational cost (see Table 1).

The FIR broadband FIB patterns by the two approaches for array with pre-steering delays are plotted in Fig. 6(c) and (d), respectively. The result on the array with pre-steering delays is somewhat similar to that on the array without pre-steering delays. The design performance of all the FIR beamformers are presented in Table 1.

8. Conclusion

Two approaches to the optimal design of FIR filters for broadband beamformers with frequency invariant patterns using second-order cone programming have been proposed. The first one is a two-step method, which first designs the array weights via optimal array pattern synthesis and then designs the FIR filters. The other is a joint optimization method which designs the FIR filters directly by jointly optimizing the spatial and frequency responses. Convex SOCP-based formulations of our design problems are derived. We illustrate the proposed approaches by applying them to a semicircular hydrophone array. Results of computer simulations and lake experiment show good performance of the proposed approaches. The beam responses obtained by the ''two-step method'' is approximately constant over one-octave frequency bandwidth. The drawback of this method is that the sidelobes at transition band and the beam responses magnitude at stopband are difficult to be specified. The joint optimization method can provide the global optimum solution to FIR broadband FIB. It provides higher design precision in mainlobe areas over the passband as compared to the ''two-step method'' and guarantees that the sidelobes at the transition band and beam responses magnitude in the stopband are strictly below the prescribed threshold value. The joint optimization method shows superior performance at the cost of increased amount of computation.

References

[1] Ward DB, Kennedy RA, Williamson RC. Theory and design of broadband sensor arrays with frequency invariant far-field beam patterns. J Acoust Soc Am 1995;97(2):1023–34.

[2] Ward DB, Kennedy RA, Williamson RC. FIR filter design for frequency invariant beamformers. IEEE Signal Proc Lett 1996;3(3):69–71.

[3] Frost III OL. An algorithm for linearly constrained adaptive array processing. Proc IEEE 1972;60(8):926–35.
[4] Compton Jr RT. The relationship between tapped delay-line and FFT processing in adaptive arrays. IEEE Trans Antennas Propagat 1988;36(1):15–26.
[5] Godara LC. Application of the fast fourier transform to broadband beamforming. J Acoust Soc Am 1995;98(1):230–40.
[6] Zhang YW, Ma YL. An efficient architecture for real-time narrowband beamforming. IEEE J Oceanic Eng 1994;19(4):635–8.
[7] Dolph CL. A current distribution for broadside arrays which optimizes the relationship between beamwidth and sidelobe level. Proc IRE 1946;34(6):335–48.
[8] Nordebo S, Zang Zhuquan, Claesson I. A semi-infinite quadratic programming algorithm with applications to array pattern synthesis. IEEE Trans Circuits Systems II 2001;48(3):225–32.
[9] Ng BP, Er MH, Kot C. A flexible array synthesis method using quadratic programming. IEEE Trans Antennas Propagat 1993;41(11):1541–50.
[10] Wu L, Zielinski A. Equivalent linear array approach to array pattern synthesis. IEEE J Ocean Eng 1993;18(1):6–14.
[11] Wu L, Zielinski A. An iterative method for array pattern synthesis. IEEE J Ocean Eng 1993;18(3):280–6.
[12] Zhou PY, Ingram MA. Pattern synthesis for arbitrary arrays using an adaptive array method. IEEE Trans Antennas Propagat 1999;47(5):862–9.
[13] Lebret H, Boyd S. Antenna array pattern synthesis via convex optimization. IEEE Trans Signal Process 1997;45(3):526–32.
[14] Wang F, Balakrishnan V, Zhou PY, Chen JJ, Yang R, Frank C. Optimal array pattern synthesis using semidefinite programming. IEEE Trans Signal Proces 2003;51(5):1172–83.
[15] Lobo M, Vandenberghe L, Boyd S, Hebret H. Applications of second-order cone programming. Linear Algebra Appl 1998;248(1–3):193–228.
[16] Vorobyov SA, Gershman AB, Luo ZQ. Robust adaptive beamforming using worst-case performance optimization: a solution to the signal mismatch problem. IEEE Trans Signal Proces 2003;51(2):313–24.
[17] Yan SF, Ma YL. Robust supergain beamforming for circular array via second-order cone programming. Appl Acoust 2005;66(9):1018–32.
[18] Liu J, Gershman AB, Luo ZQ, Wong KM. Adaptive beamforming with sidelobe control: a second-order cone programming approach. IEEE Signal Proces Lett 2003;10(11):331–4.
[19] Toh KC, Todd MJ, Tutuncu RH. SDPT3 – a Matlab software package for semidefinite programming. Optim Meth Softw 1999;11-12:545–81.
[20] Sturm JF. Using SeDuMi 1.02, a MATLAB toolbox for optimization over symmetric cones. Optim Meth Softw 1999;11–12:625–53.
[21] Chen X, Parks T. Design of FIR filters in the complex domain. IEEE Trans Acoust, Speech, Signal Proces 1987;35(2):144–53.
[22] Zhang X, Dai S. Designs of Chebyshev-type complex FIR filters and digital beamformers with linear-phase characteristics. IEE Proc Vision, Image Signal Proces 1994;141(1):2–8.
[23] Zhu WP, Ahmad MO, Swamy MNS. A new approach for weighted least-square design of FIR filters. In: Proc. ISCAS '99; 1999. p. 267–70.
[24] Burrus CS, Barreto JA, Selesnick IW. Iterative reweighted least-squares design of FIR filters. IEEE Trans Signal Proces 1994;42(11):2926–36.
[25] Lang M, Bamberger J. Nolinear phase FIR filter design according to the L_2 norm with constraints for the complex error. Signal Proces 1994;36(1):31–40.
[26] Dam HH, Teo KL, Nordebo S, Cantoni A. The dual parameterization approach to optimal least square FIR filter design subject to maximum error constraints. IEEE Trans Signal Proces 2000;48(8):2314–20.
[27] Adams JW. FIR digital filters with least-squares stopbands subject to peak-gain constraints. IEEE Trans Circuits Syst 1991;39(4):376–88.
[28] Lu WS. Design of nonlinear-phase FIR digital filters: a semidefinite programming approach. In: Proc. ISCAS'99; 1999. p. 263–6.
[29] Yan SF, Ma YL. A unified framework for designing FIR filters with arbitrary magnitude and phase response. Digital Signal Process 2004;14(6):510–22.
[30] Yan SF, Ma YL. Design of FIR beamformer with frequency invariant patterns via jointly optimizing spatial and frequency responses. In: Proc. ICASSP 2005, Philadelphia, US: 4; 2005. p. 789–92.
[31] Yan SF, Ma YL. Frequency invariant beamforming via jointly optimizing spatial and frequency responses. Prog Nat Sci 2005;15(4):368–74.

[32] Nesterov Y, Nemirovsky A. Interior-point polynomial methods in convex programming, volume 13 of Studies in Applied Mathematics. Philadelphia, PA: SIAM; 1994.
[33] Cox H, Zeskind RM, Owen MH. Robust adaptive beamforming. IEEE Trans Acoust Speech, Signal Process 1987;35(1):1365–76.
[34] Wu RB, Ma YL, James RD. Array pattern synthesis and robust beamforming for a complex sonar system. IEE Proc Radar, Sonar Navig 1997;144(6):370–6.

Shefeng Yan was born in Hubei Province, P.R.China, in 1978. He received the B.S., M.S., and Ph.D. degrees all in electrical engineering from Northwestern Polytech. Univ. (NPU), Xi'an, China, in 1999, 2001 and 2005, respectively.

He is currently a post-doctoral fellow with the Institute of Acoustics, Chinese Academy of Sciences, Beijing, China. His current research interests include array signal processing, robust adaptive beamforming, high-resolution direction-of-arrival estimation, and signal processing applications to underwater acoustics, radar, and wireless mobile communication systems.

Dr. Yan is a member of the IEEE, as well as a member of the Acoustical Society of China.